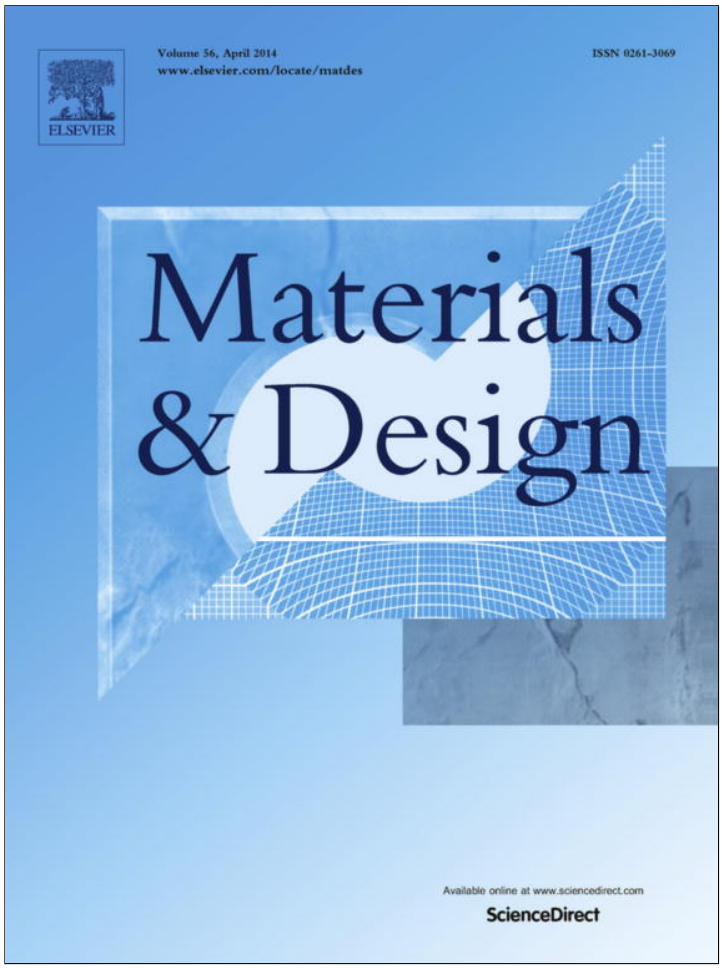

Materials and Design 56 (2014) 731–739

Contents lists available at ScienceDirect

Materials and Design

journal homepage: www.elsevier.com/locate/matdes

Compressive efficiency of stretch–stretch-hybrid hierarchical composite lattice cores

Sha Yin [a,b,*], Linzhi Wu [b,*], Steven R. Nutt [c]

[a] International Research Center for Biological & Nature-Inspired Materials, Beihang University, Beijing 100191, China
[b] Center for Composite Materials, Harbin Institute of Technology, Harbin 150001, China
[c] Department of Chemical Engineering and Materials Science, University of Southern California, Los Angeles, CA 90089-0241, USA

ARTICLE INFO

Article history:
Received 29 November 2012
Accepted 9 November 2013
Available online 21 November 2013

Keywords:
Lattice materials
Carbon fiber
Hierarchy
Structural efficiency
Optimization

ABSTRACT

Composite lattice cores featuring structural hierarchy were developed to achieve greater buckling resistance. The stretch–stretch-hybrid hierarchical lattice cores were fabricated with a two-step approach by assembling composite pyramidal lattice (CPL) sandwiches into macroscopic truss configurations. Analysis and experiments were performed to determine the out-of-plane compressive strength. Hierarchical CPL cores were evaluated based on their failure mechanism maps, and the structural efficiency was affected by the ratio of strut length at different scales (e.g. L/l_1). With the specific limited L/l_1, the optimized hierarchical CPL core was almost 5 times stronger than lower-order CPL cores with rectangular trusses (at relative density 0.01). The fully optimized hierarchical CPL cores can be as efficient as optimized CPL cores with hollow trusses. Effects of topologies at two different length scales on the performance of hierarchical structures were also assessed.

1. Introduction

Lattice materials are widely regarded as efficient, stretch-dominated structures well-suited for multifunctional applications, and can be produced from metals, polymers, or composites [1–3]. Metallic lattice structures have been produced with a variety of topologies such as tetrahedral [4], pyramidal [5] and Kagome [6]. Composite lattices can also be produced in various configurations, and exhibit specific properties superior to their metallic counterparts, allowing designers to fill gaps in the material property space. Because of the intrinsic hierarchical nature of composites on small length scales (10–20 μm) [7], composite lattices are assumed as hierarchical structures that can be analyzed from the materials level up to the structural level [8]. In weight-sensitive designs, ultralightweight composite lattices are susceptible to buckling, which can limit their eligibility for certain applications.

Through design of the truss members, several composite truss structures have been explored, including a hollow composite pyramidal lattice (CPL) core [9], a hybrid truss CPL concept [10] and CPL cores with foam sandwich struts [11]. To produce hollow CPL cores, a thermal expansion molding technique was developed [9]. In that work, the out-of-plane compressive strength of a hollow CPL core was reportedly twice that of solid truss counterparts at ultra-low densities, where Euler buckling controls failure . The specific strength of the hollow CPL can surpass that of hollow metallic microlattices, reportedly the world's lightest structures [12].

Structural hierarchy is generally observed in natural materials (e.g., wood and bone [13,14]) and often employed in engineering structures to increase buckling strength. For engineering cellular materials, several hierarchical structures have also been developed, including a self-similar hierarchical corrugated sandwich core [15], a corrugated sandwich core with foam sandwich struts [16], and a hierarchical honeycomb core [17]. The self-similar hierarchical corrugated core is reportedly 10 times stronger than that of the lower-order corrugated core of equivalent relative density [15]. However, it is generally difficult and costly to fabricate hierarchical structures directly, especially with periodic cellular materials, due to the different length scales that must be controlled and assembled simultaneously.

The scope of the present study is to increase the buckling resistance and the specific compressive strength of traditional lattice structures by employing structural hierarchy. Extended hierarchical constructions based on carbon fiber reinforced composite lattice cores are developed using a two-step fabrication approach. Specially, a protocol is outlined to evaluate efficiencies of these complex structures based on the flowchart presented in Fig. 1. By following the protocol, both analysis and experiments are carried out, and the newly developed structures are compared with competing constructions. Effects of topology or shape variation at

* Corresponding authors. Present address: International Research Center on Biological & Nature-Inspired Materials, Beihang University, Beijing 100191, China (S. Yin). Tel.:+86 10 82316326; fax: +86 10 82317108.
E-mail addresses: yinsha2008@gmail.com (S. Yin), wlz@hit.edu.cn (L. Wu).

0261-3069/$ - see front matter © 2013 Elsevier Ltd. All rights reserved.
http://dx.doi.org/10.1016/j.matdes.2013.11.012

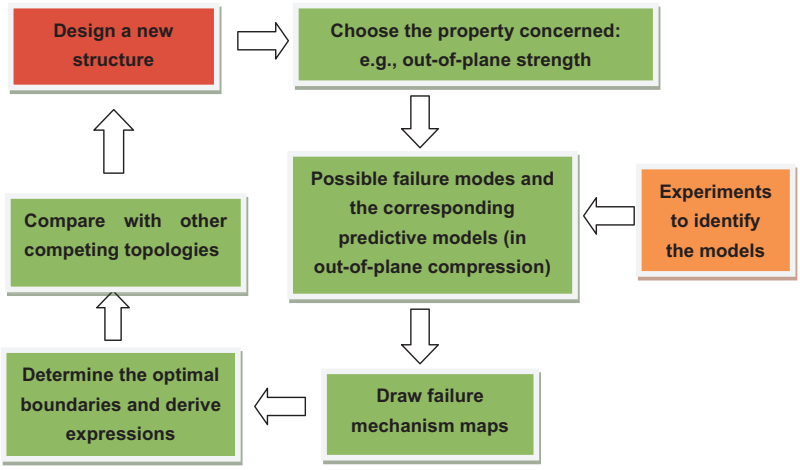

Fig. 1. A protocol guiding structural design.

different length scales on the structural performance are also assessed and discussed.

2. Illustration and analysis of a hierarchical CPL core construction

A schematic illustrating the procedure used to build hierarchical periodic structures is shown in Fig. 2a. A hierarchical pyramidal lattice core was assembled from hollow CPL sandwiches. Ignoring the hierarchy of the parent materials (fiber composites), the hierarchical structures developed here can be considered to be of order 2. The macroscopic core is a pyramidal lattice core with rectangular struts, while the individual rectangular struts are mesoscopic sandwich beams with hollow CPL truss cores. The relative density $\bar{\rho}'$ of the hierarchical CPL core, can be expressed as

$$\bar{\rho}' = \frac{2(2Lwt_f + \bar{\rho}_h Lwl_1 \sin\omega)}{L\sin\omega'[L\cos\omega' + w + (2t_f + l_1\sin\omega)/\sin\omega']^2} \quad (1)$$

where geometrical dimensions of the sandwich strut L, w, t_f, ω' and those of lattice strut of the hollow CPL core l_1, d_o, d_i, ω are defined in Fig. 2a, and $\bar{\rho}_h$ represents the relative density of the hollow CPL cores in the sandwich strut. Note that in this expression, the

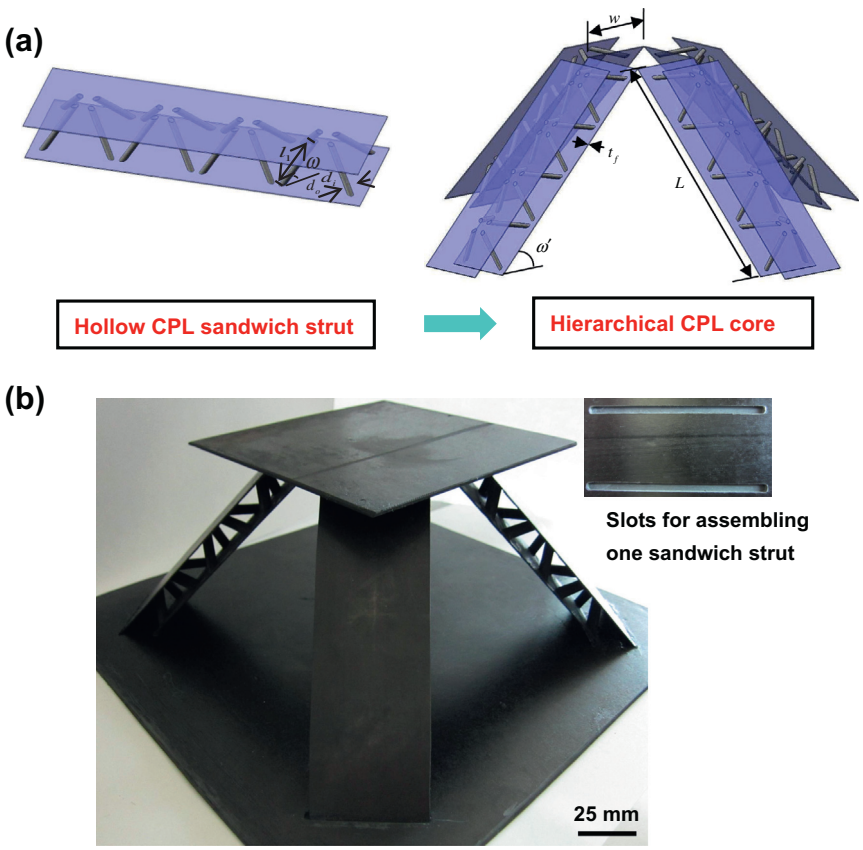

Fig. 2. (a) Illustration for building hierarchical periodic structures: from composite pyramidal lattice (CPL) core sandwich to hierarchical CPL core and (b) prototypical hierarchical CPL core sandwich structure.

difference in unidirectional and woven prepreg density is considered to be negligible.

Through-thickness compressive strength is an important property for this new hierarchical construction. Indeed, the flowchart in Fig. 1 dictates the initial step of mechanical property analysis in out-of-plane compression. Theoretical prediction is carried out for the compression strength of the hierarchical CPL core by analyzing the deformation of a single sandwich strut. Analysis is based on the theory of sandwich structures, as shown in Fig. 3, assuming that the sandwich struts have clamped boundary conditions.

2.1. Stiffness

For an imposed displacement δ in the z-direction, considering bending deformations other than stretching, the axial and shear force, F'_a and F'_s, in the sandwich strut are given as

$$F'_a = \frac{\delta \sin\omega'}{L} A_{sand} \tag{2}$$

$$F'_s = \frac{12\delta \cos\omega'}{L^3} D_{sand} \tag{3}$$

where A_{sand} and D_{sand} are the compressive and bending stiffnesses of the sandwich strut, respectively. $A_{sand} = 2E_f^{eq} w t_f$ and $D_{sand} = \frac{1}{2}E_f^{eq} w t_f l_1^2 \sin^2\omega$, where E_f^{eq} is the equivalent compressive modulus of the laminated face sheets in the sandwich strut. The total force F' in the z-direction follows as

$$F' = F'_a \sin\omega' + F'_s \cos\omega' = \delta\left[\frac{\sin^2\omega'}{L} A_{sand} + \frac{12\cos^2\omega'}{L^3} D_{sand}\right] \tag{4}$$

The effective nominal compressive stiffness of the hierarchical CPL cores is given by

$$\begin{aligned} E' &= \left[A_{sand}\sin^2\omega' + \tfrac{12D_{sand}}{L^2}\cos^2\omega'\right] \frac{2\sin\omega'}{[L\cos\omega' + w + (2t_f + l_1\sin\omega)/\sin\omega']^2} \\ &= \bar{\rho}'\left(E_f^{eq}\sin^4\omega' + 3E_f^{eq}\tfrac{l_1^2\sin^2\omega}{L^2}\sin^2\omega'\cos^2\omega'\right)/\left(1 + \bar{\rho}_h\tfrac{l_1\sin\omega}{2t_f}\right) \end{aligned} \tag{5}$$

The hollow CPL core contributes little to the out-of-plane stiffness of the hierarchical CPL core. Thus, the specific stiffness decreases with increasing structural hierarchy, a finding that is consistent with theoretical predictions [7].

2.2. Collapse modes and strength predictions

Six competing failure modes are considered for the hierarchical CPL core subjected to out-of-plane compression. The failure modes are analyzed from element level to higher structural orders, and present analytical predictions for the corresponding collapse loads.

2.2.1. Fracture of hollow truss

Sandwich columns of length L form larger struts of the hierarchical CPL core (Fig. 2b). Accordingly, shear forces in the sandwich strut can trigger failure of hollow trusses that form the hollow CPL core. Fracture of a hollow truss implies that the peak shear force for a unit cell of the sandwich strut is

$$F'_s = \pi(d_o^2 - d_i^2)\sigma_{sh}\left[\sin\omega + \frac{3}{4}\frac{d_o^2 + d_i^2}{l_1^2}\frac{\cos^2\omega}{\sin\omega}\right] \tag{6}$$

where σ_{sh} is the fracture strength of hollow trusses. From Eqs. (2) and (3), the relationship between F'_a and F'_s can be determined. Then using Eq. (4), the strength of the hierarchical composite pyramidal core is given as

$$\begin{aligned} \sigma'_p = {} & \frac{2\pi(d_o^2 - d_i^2)\sigma_{sh}}{[L\cos\omega' + w + (2t_f + l_1\sin\omega)/\sin\omega']^2}\left[\sin\omega + \frac{3}{4}\frac{d_o^2 + d_i^2}{l_1^2}\frac{\cos^2\omega}{\sin\omega}\right] \\ & \times \left[\cos\omega' + \frac{\sin^2\omega'}{\cos\omega'}\frac{A_{sand}L^2}{12D_{sand}}\right] \end{aligned} \tag{7}$$

2.2.2. Euler buckling of a hollow truss

Alternatively, if elastic Euler buckling of the smaller hollow trusses occurs, the peak shear force in the sandwich strut is given as

$$F'_s = \frac{\pi^2 E_{sh}^{eq}\left(d_o^4 - d_i^4\right)}{4l_1^2}\left[\sin\omega + \frac{3}{4}\frac{d_o^2 + d_i^2}{l_1^2}\frac{\cos^2\omega}{\sin\omega}\right] \tag{8}$$

Thus, the collapse strength of the hierarchical composite pyramidal core is

$$\begin{aligned} \sigma'_p = {} & \frac{\pi^2 E_{sh}^{eq}\left(d_o^4 - d_i^4\right)}{2l_1^2[L\cos\omega' + w + (2t_f + l_1\sin\omega)/\sin\omega']^2}\left[\sin\omega + \frac{3}{4}\frac{d_o^2 + d_i^2}{l_1^2}\frac{\cos^2\omega}{\sin\omega}\right] \\ & \times \left[\cos\omega' + \frac{\sin^2\omega'}{\cos\omega'}\frac{A_{sand}L^2}{12D_{sand}}\right] \end{aligned} \tag{9}$$

2.2.3. Face sheet wrinkling of a sandwich strut

The laminated face sheets of a sandwich column subjected to axial compression wrinkle when the face sheets are relatively thin. In such cases, the maximum load causing wrinkling of the inclined sandwich strut can be expressed as $F'_a = P_{fw}$. Hence, the strength of the hierarchical composite pyramidal core is

$$\begin{aligned} \sigma'_p = {} & \frac{16\pi^2 D_f}{\left(\sqrt{2}l_1\cos\omega + l_2\right)^2} \\ & \times \frac{\left[\sin\omega' + \frac{\cos^2\omega'}{\sin\omega'}\frac{12D_{sand}}{L^2A_{sand}}\right]}{[L\cos\omega' + w + (2t_f + l_1\sin\omega)/\sin\omega']^2} \end{aligned} \tag{10}$$

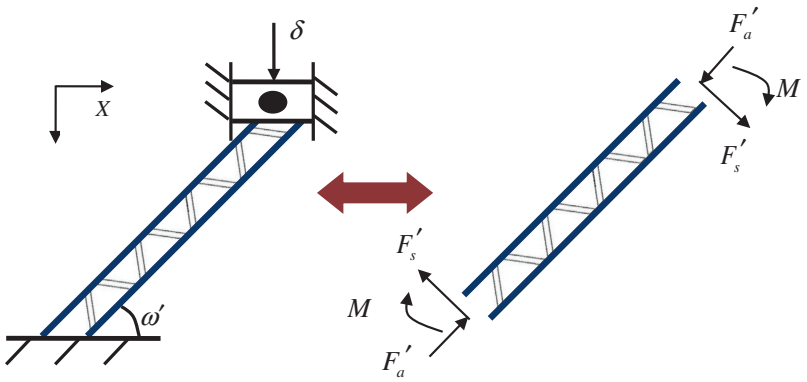

Fig. 3. Analysis for one sandwich strut of hierarchical CPL cores in out-of-plane compression.

2.2.4. Face sheet crushing of a sandwich strut

Sandwich struts with face sheets of thickness t_f for the macroscopic CPL can fail by face sheet crushing when subjected to compressive loads. The force component along the sandwich strut is $F'_a = P_{fc}$, and thus the collapse strength of the hierarchical composite pyramidal core with sandwich struts is

$$\sigma'_p = 4\sigma_f t_f w \frac{\left[\sin\omega' + \frac{\cos^2\omega'}{\sin\omega'}\frac{12D_{sand}}{L^2A_{sand}}\right]}{\left[L\cos\omega' + w + (2t_f + l_1\sin\omega)/\sin\omega'\right]^2} \tag{11}$$

where σ_f is the crushing strength of the face sheets of the sandwich struts.

2.2.5. Euler macrobuckling of a sandwich strut

Under compressive load, Euler buckling can occur when the strut is slender. The sandwich beams are assumed as built-in Euler beams, and thus the compressive collapse load along the sandwich column is specified by $F'_a = P_{eb}$. The compressive strength of the hierarchical composite pyramidal core is given by

$$\sigma'_p = 8\pi^2\frac{D_{sand}}{L^2}\frac{\left[\sin\omega' + \frac{\cos^2\omega'}{\sin\omega'}\frac{12D_{sand}}{L^2A_{sand}}\right]}{\left[L\cos\omega' + w + (2t_f + l_1\sin\omega)/\sin\omega'\right]^2} \tag{12}$$

2.2.6. Shear macrobuckling of a sandwich strut

Shear buckling of the sandwich struts is controlled by the shear stiffness of the hollow CPL core, and occurs at a load $F'_a = P_{sb}$. Thus, the compressive failure strength in this mode is given by

$$\sigma'_p = \frac{1}{4}E_{sh}^{eq}\bar{\rho}_h w l_1 \times \sin\omega\sin^2 2\omega\frac{\left[\sin\omega' + \frac{\cos^2\omega'}{\sin\omega'}\frac{12D_{sand}}{L^2A_{sand}}\right]}{\left[L\cos\omega' + w + (2t_f + l_1\sin\omega)/\sin\omega'\right]^2} \tag{13}$$

2.3. Collapse mechanism maps

Collapse mechanism maps illustrate the regimes of the dominant failure modes for hierarchical CPL cores. To construct such maps, the operative failure mode in out-of-plane compression is assumed the one for which the strength is lowest. Fig. 5a–c shows examples of mechanism maps, which are constructed as a function of face sheet parameters t_f/l_1 and L/l_1 for different d_i/l_1 with structural dimensions $d_o/l_1 = 0.3$, $w/l_1 = 2.5$ and inclined angle $\omega = \omega' = 45^\circ$. The compressive properties of the elementary face sheets and hollow trusses are shown in Table 1. Because the core density is relatively low for $d_i/l_1 = 0.27$ (Fig. 5a), shear buckling is expected to dominate over most of the design space, and face sheet crushing is unlikely. Hollow truss fracture (HTF), emerges on the left side of each map (Fig. 5a–c) for cores with much shorter struts.

3. Experiments

3.1. Specimen fabrication

In the present study, the hierarchical CPL cores with hollow CPL sandwich struts were fabricated in two steps. First, hollow CPL core sandwich structures were manufactured using the thermal expansion molding technique with assembled steel molds and silicone rubber [9]. After inserting rubber-core composite trusses into the holes of the steel molds and stacking prepregs on their top and bottom surfaces, the whole assembly was cured at 125 °C for 2 h. Then, hollow CPL sandwich beams were obtained as steel molds and rubber were removed. Then, four hollow CPL sandwich beams of width $w = 50$ mm were positioned at an inclination angle $\omega' = 45^\circ$ with respect to the base of the unit cell forming the hierarchical CPL cores. The higher-order CPL core as shown in Fig. 2b, consisting of a single unit cell, was attached to two laminated face sheets featuring recesses to receive the struts. Prior to compression testing, a low-viscosity epoxy adhesive was applied to the sandwich struts ends and around the slots to create fixed boundary conditions. Representative samples with selected dimensions were designed and fabricated for compression. The selection of sample dimensions in the present study was also restricted by the maximum size of the bottom face sheet (Fig. 2b) that could be fabricated in the laboratory.

3.2. Out-of-plane compression

Through-thickness compression tests of hierarchical CPL sandwich structures were performed at a displacement rate of 0.5 mm/min using a screw-driven testing machine (INSTRON 5569). For specimen A ($\bar{\rho}' = 1.11\%$), $L = 100$ mm, $t_f = 0.71$ mm $d_i = 4.5$ mm. The measured compressive response is plotted in Fig. 6a. The nominal stress increased almost linearly with the nominal strain and reached a peak stress 0.27 MPa (0.29 MPa as predicted), at which point face sheet wrinkling occurred in at least one of the four large sandwich struts, manifest as a sharp drop in supported load. Subsequently, a series of local buckling events occurred between the points of attachment to the pyramidal truss core. The failure modes of the hierarchical CPL core occurred in both 1–3 and 2–4 directions at an applied strain $\varepsilon \approx 0.03$, as shown in Fig. 6b. As strain increased, node rupture of the small hollow trusses was observed, much like hollow CPL sandwich columns loaded in edgewise compression [8]. The measured failure loads for Specimen A differed from predicted values by only 6.9%.

Considering shear buckling as a primary failure mode for the hierarchical pyramidal core with four inclined sandwich struts, samples were also designed to identify this failure mode. For Specimen B, ($\bar{\rho}' = 1.06\%$), $L = 150$ mm, $t_f = 1.12$ mm $d_i = 5.4$ mm. The measured collapse behavior for Specimen B is presented in Fig. 7a, along with photographs showing the failure mode at a strain $\varepsilon \approx 0.035$. The measured strength was 0.33 MPa, and the predicted value (SB) was 0.42 MPa. The deviation was about 25% and failure mode for the 1–3 direction (arrow) was not symmetrical, an observation that was attributed to variability in the sandwich beams and boundary condition sensitivity created by the adhesive. However, the prediction models in Section 2 related to the expressions in [8] were shown to be reliable. Note that for failure modes indicated in Fig. 4a and b (failure of hollow trusses in the sandwich struts), specimens were impossible to fabricated here.

4. Optimization of the hierarchical CPL core

The specific strength of the hierarchical CPL core at a given relative density can be maximized by adjusting dimensions. The optimization problem is based on the collapse mechanism maps, where the following restrictions are applied:

(1) The stacking sequence of the laminated face sheet is specified as [0/90/0], while that of the laminated shell (hollow truss) is [(0,90)].
(2) The inclination angles of CPL cores at two different length scales are equal and the choice $\omega = \omega' = 45^\circ$, which is optimal to maximize both compressive and shear strengths, as indicated in previous literature [18].
(3) Lattice geometries are constrained in practice by the steel molds employed in the fabrication section, and thus $d_o/l_1 = 0.3$, $l_2/l_1 = 0.75$, $w/l_1 = 2.5$.

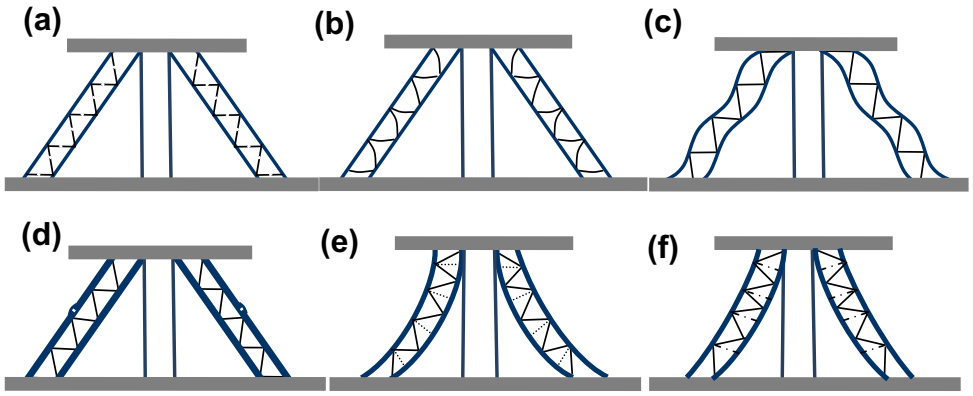

Fig. 4. Possible failure modes for the hierarchical CPL core in out-of-plane compression: (a) truss fracture, (b) truss buckling, (c) face sheet wrinkling of sandwich struts, (d) face sheet crushing of sandwich struts, (e) Euler buckling of sandwich struts (note that the center lines will deform with the sandwich struts) and (f) shear buckling of sandwich struts.

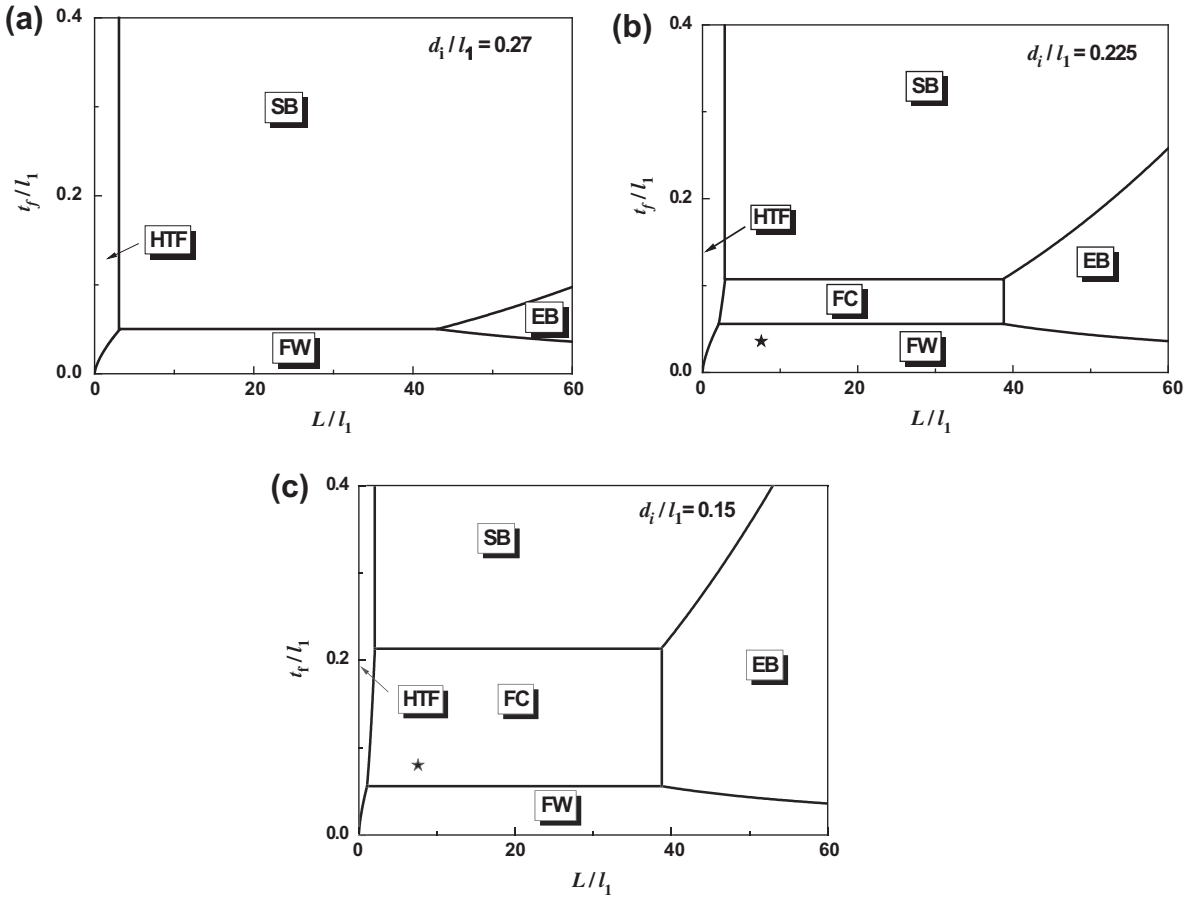

Fig. 5. Failure mechanism maps for the hierarchical CPL sandwich structure in out-of-plane compression constructed as a function of face sheet parameters t_f/l_1 and L/l_1 for: (a) $d_i/l_1 = 0.27$, (b) $d_i/l_1 = 0.225$, and (c) $d_i/l_1 = 0.15$. (SB = shear buckling; FW = face sheet wrinkling; FD = face sheet delamination; EB = Euler buckling; HTF = hollow truss fracture).

Collapse mechanism maps for out-of-plane compression are constructed as functions of t_f/l_1 and d_i/l_1, as shown in Fig. 8 (truss stacking is chosen as [(0,90)]). The governing failure modes for a specific $L/l_1 = 2.5$ are hollow truss fracture (HTF) and face sheet crushing (FC), as shown in Fig. 8a, while shear buckling (SB) and face sheet crushing (FC) of sandwich struts are dominant for $L/l_1 = 7.5$ (Fig. 8b). Contours of normalized strength $\bar{\sigma} \equiv \sigma'_p/\sigma_f$ and relative density $\bar{\rho}'$ are added to the maps to convey structural properties associated with the failure mode transitions. The optimal designs that maximize the compressive strength for any given relative density should lie along the boundaries of the collapse regimes, where two failure modes are equally likely, and the arrows

Table 1
Mechanical properties of composite elements.

Laminated face sheet			Stacking sequence	E_f^{eq} (GPa)	σ_f (MPa)
			[0/90/0]	41.2	135.8
Hollow truss					
d_o (mm)	d_i (mm)	$\bar{\rho}_h$ (%)	Stacking sequence	E_{sh}^{eq} (GPa)	σ_{sh} (MPa)
6	5.4	1.07	[(0,90)]	10.15	93.11
6	4.5	2.21	[0_2/(0,90)]	11.66	121.32
6	3	4.53	[0_4/$(0,90)_2$]	13.52	188.68

shown in Fig. 8b trace the path of optimal designs. The relationship between the optimal normalized compressive strength and relative density can be formulated for the hierarchical CPL core and written as

$$\bar{\rho}' = \begin{cases} \dfrac{(2+16\sigma_f/E_{sh}^{eq})}{(1+3l_1^2/2L^2)}\bar{\sigma}', & \text{FC—SB} \\ \dfrac{4\sqrt{2}\frac{w}{L}}{\left(\frac{\sqrt{2}}{2}+\frac{w}{L}+\frac{l_1}{L}\right)^2}\left(\dfrac{3\sigma_f\left(1+\frac{l_1}{l_2}\right)^2\left(\frac{\sqrt{2}}{2}+\frac{w}{L}+\frac{l_1}{L}\right)^2}{2\sqrt{2}\pi^2E_f^{eq}\left(\frac{l_2^2}{l_1^2}+\frac{3}{2}\right)}\right)^{1/3}\bar{\sigma}'^{1/3}+\dfrac{16\sigma_f}{E_{sh}^{eq}\left(1+\frac{3l_1^2}{2L^2}\right)}\bar{\sigma}', & \text{FW—SB} \end{cases} \quad (14)$$

The objective of the optimal design is to select (t_f/l_1, d_i/l_1) for a prescribed L/l_1 that maximizes the compressive strength. The relative density is plotted as a function of strength for different L/l_1 in Fig. 9a. For low L/l_1, where HTF occurs, the relative density is much greater at a given strength than for high L/l_1, where SB occurs. Thus, an optimally designed structure cannot fail by HTF.

The plots for L/l_1values where SB occurs are also enlarged in Fig. 9b, which shows that the FW–SB boundary with higher L/l_1 yields maximum strength at a given relative density, while the FC–SB line yields maximum strength with lower L/l_1. The map indicates that the strength of the hierarchical CPL core can be further increased by judicious selection of L/l_1. However, the maximum value of L/l_1 is limited in the present study to 12.5 attributed to lab condition. The fully optimized structure can be obtained when all possible failure modes are designed to happen at the same time shown as the dashed dot black line in Fig. 9b.

5. Structural efficiency evaluation by comparison with other structures

Structural efficiency here is defined as the peak strength at a given relative density. The featured CPL core described above is a non-self-similar hierarchical structure. To assess this structural

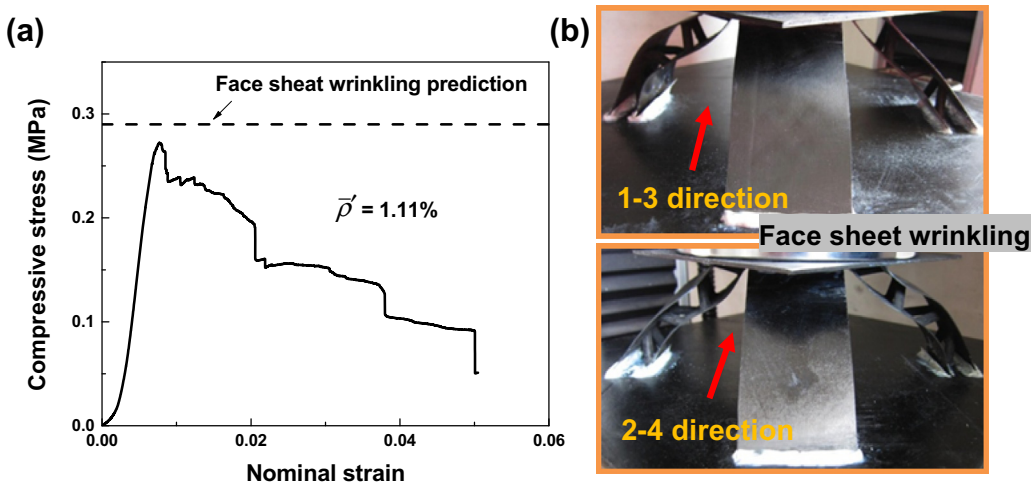

Fig. 6. (a) Measured compression response of specimen A (the analytical prediction of the collapse stress is also included) and (b) representative failure modes of the sandwich struts.

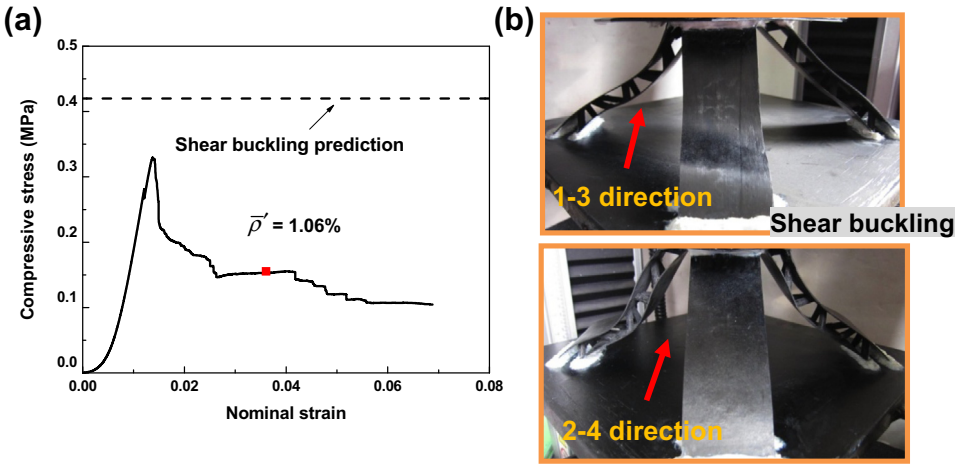

Fig. 7. (a) Measured compression response of specimen B (the analytical prediction of the collapse stress is also included) and (b) representative failure modes of the sandwich struts.

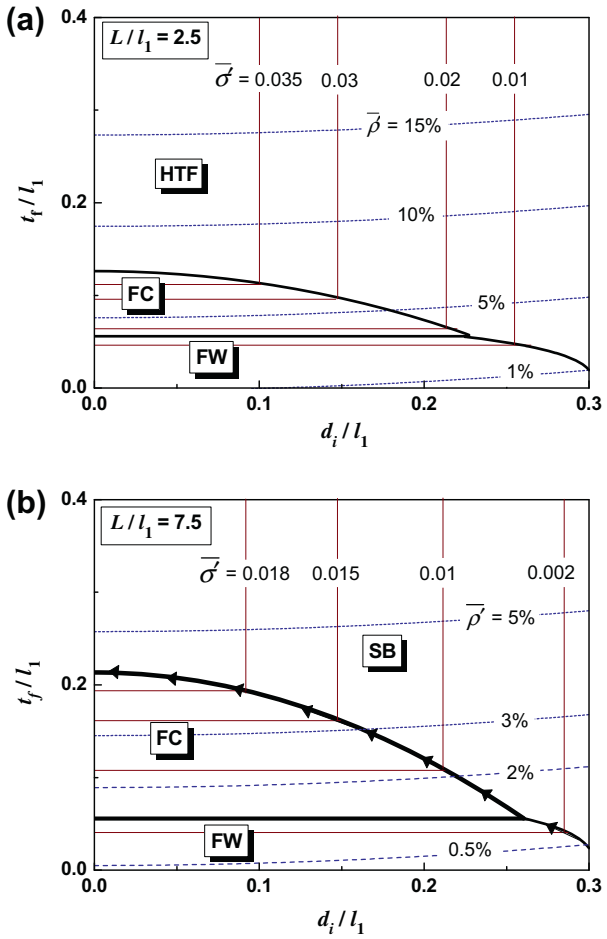

Fig. 8. Collapse mechanism maps with (a) $L/l_1 = 2.5$ and (b) $L/l_1 = 7.5$. Note that the arrows in (b) designate the path of optimum designs with increasing relative density $\bar{\rho}'$.

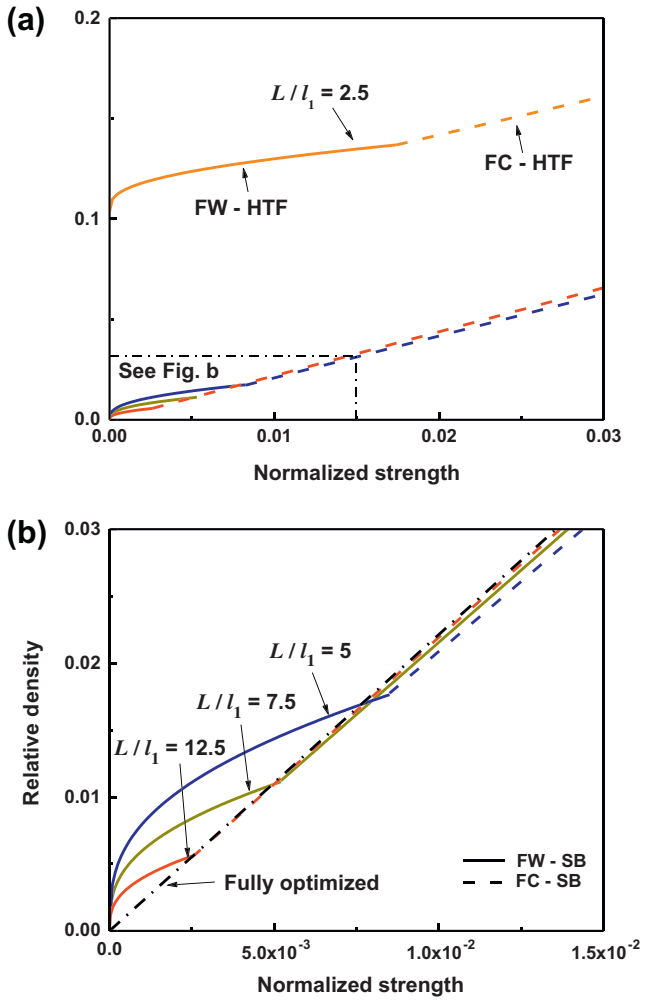

Fig. 9. (a) Normalized strength for the hierarchical CPL cores with specific L/l_1 and (b) the enlarged drawing of (a).

design, the structural efficiency is compared to that of CPL structures of lower order. However, varying the truss spacing at the pyramidal node (l_2 for hollow CPL and w for the hierarchical CPL) will result in different compressive strength decrements (knock-down coefficients) for different structures. Therefore, these effects are eliminated by setting all node spacing to zero before comparison.

5.1. Comparison to lower-order CPL cores with round trusses

After setting $l_2 = 0$, the hierarchical CPL cores are first compared to non-hierarchical CPL cores with solid/hollow round trusses, and the results are summarized in Fig. 10a. Note that solid trusses are assumed to have compressive properties equivalent to those of hollow trusses shown in Table 1, and all the strengths are divided by face sheet compressive strength, σ_f, during normalization. Fig. 10a shows that hierarchical CPL cores outperform CPL cores with solid round trusses, and are more efficient than CPL cores with hollow trusses at relative density values of $\bar{\rho}' > 0.006$.

5.2. Comparison to lower-order CPL cores with rectangular (sheet-based) trusses

The key compressive index σ/E is critical to structural efficiency. Here, the index of laminates is greater than that of composite tubes. Therefore, hierarchical CPL cores mainly supported by laminates can easily outperform lower-order truss-based CPL cores. Additionally, the performance of CPL cores with rectangular trusses in Fig. 10a is considered. The results that lower-order CPLs with laminate-based trusses outperform those with tube-based trusses (when all structures fail by truss fracture), have further illustrated this point. However, in the event of Euler buckling, CPLs with rectangular trusses are less efficient than those with round trusses, primarily because of intrinsic truss shape efficiencies [19]. Thus, evaluation of composite structures will be more complicated than corresponding metallic structures because the key compressive index of metals is simply equal to the yield strain ε_y.

5.3. Comparison after homogenization of component materials

Next, the construction concepts alone will be compared, absent the design of the parent composites. To do this, assuming that all the structures are fabricated from a single solid material with the same mechanical properties (e.g., assumed to equal those of the face sheet, $\sigma_f/E_f^{eq} \approx 0.0033$), the associated strength versus relative density curves were redrawn. As shown in Fig. 10b, the hierarchical CPL core ($L/l_1 = 12.5$) is almost 5 times stronger than the corresponding CPL core with rectangular trusses (at relative density 0.01), but almost as efficient as CPLs with solid round trusses. Moreover, the fully optimized hierarchical CPL cores can be as efficient as the optimized CPL cores with hollow trusses.

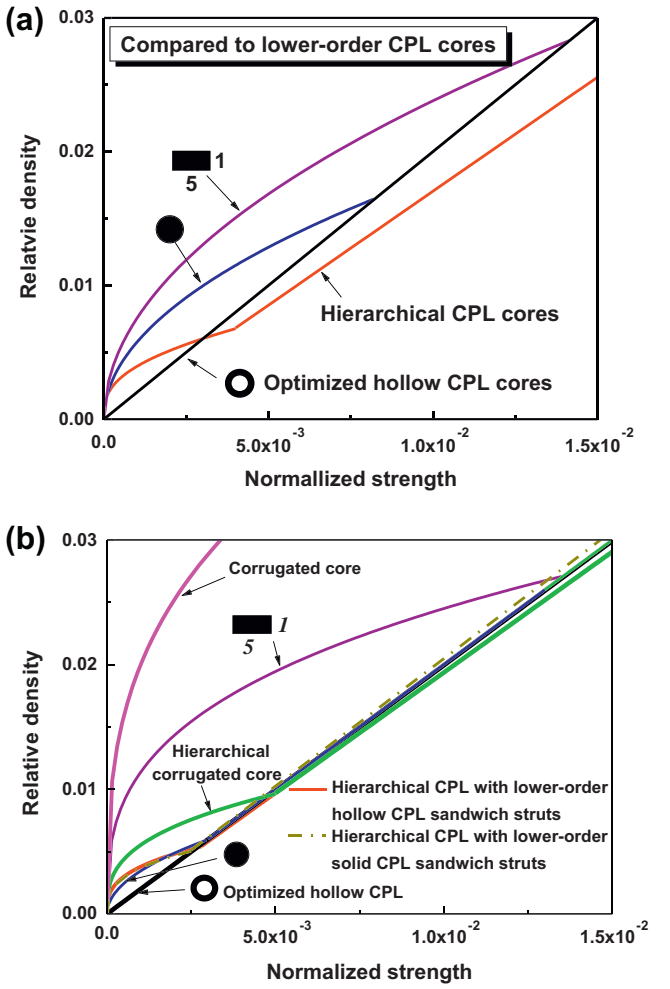

Fig. 10. Structural efficiencies of hierarchical CPL cores (a) compared to lower-order CPL cores with different trusses as shown with insets (solid/hollow round or rectangular trusses) and (b) comparison after homogenization of component materials.

5.4. Effect of macro-topology — comparison with hierarchical corrugated core

Corrugated cores are generally less efficient than lattice cores, as demonstrated in Fig. 10b. Here, the effect of macroscopic topologies on the mechanical performance of hierarchical constructions will be examined. Accordingly, hierarchical corrugated cores with hollow CPL sandwich struts were also evaluated, as shown in Fig. 11. The structures were then evaluated by following the same protocol used previously. Based on the analysis for hierarchical CPL cores, failure mechanism maps for hierarchical corrugated cores were constructed, as shown in Fig. 11, and the failure modes boundaries were identical to those shown in Fig. 8b. The similarity arises because the loading and boundary conditions of the individual struts are identical for the two kinds of structures. However, the relationship between optimized strength and relative density was different from the FW–SB section in Eq. (14), and is expressed as:

$$\bar{\rho} = \begin{cases} \frac{(2+16\sigma_f/E_{sh}^{eq})}{(1+3l_1^2/2L^2)}\bar{\sigma}, & FC-SB \\ 4\frac{L^2}{l_1^2}\frac{1}{(1+\sqrt{2}l_1/L)}\left(\frac{3\sigma_f(1+\sqrt{2}l_1/L)}{2\pi^2 E_f^{eq}(L^2/l_1^2+3/2)}\right)^{1/3}\bar{\sigma}^{1/3} + \frac{16\sigma_f}{E_{sh}^{eq}(1+3l_1^2/2L^2)}\bar{\sigma}, & FW-SB \end{cases} \quad (15)$$

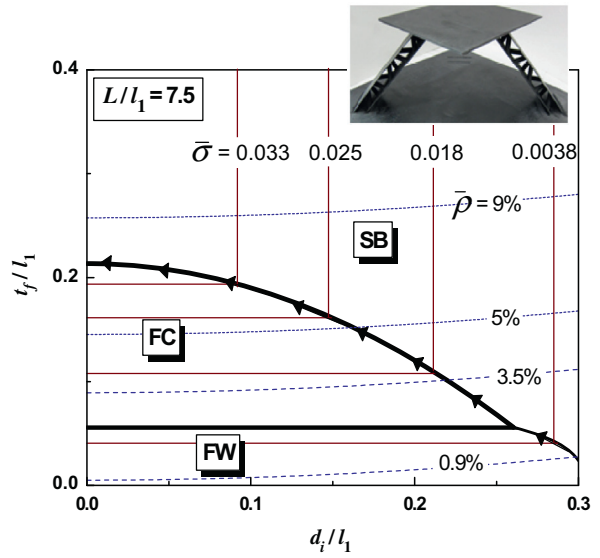

Fig. 11. Collapse mechanism maps of hierarchical corrugated core with hollow CPL sandwich struts of $L/l_1 = 7.5$.

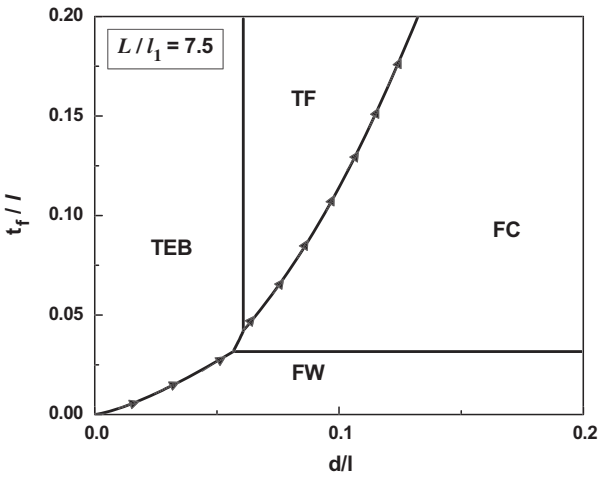

Fig. 12. Collapse mechanism map of hierarchical CPL cores assembled from CPL sandwich struts with solid trusses (TEB = truss Euler buckling; TF = Truss fracture).

The compressive strength value of hierarchical corrugated cores ($L/l_1 = 12.5$) is added to Fig. 10b (green line)[1] and compared with hierarchical CPL cores. The FW–SB section of the hierarchical corrugated core is less efficient than that of the hierarchical CPL core. Accordingly, it is concluded that the efficiency of structure at the macroscopic length scale will directly affect that of the corresponding hierarchical construction.

5.5. Effect of meso-shape

Consider hierarchical CPL cores consisting CPL sandwich struts with solid trusses (instead of hollow trusses in previous sections). The mechanism maps are constructed as shown in Fig. 12 with the same procedure, and optimization boundaries are indicated by the arrows. The expressions for optimized boundaries (omitted here for brevity) are deduced and the relationship is incorporated into

[1] For interpretation of color in Fig. 10, the reader is referred to the web version of this article.

Fig. 10b. The comparison in the figure shows that the optimized hierarchical cores assembled here from non-strengthened solid CPL sandwich struts are as efficient as those assembled from hollow CPL sandwich struts. The finding indicates that the mesoscopic truss shape has little effect on the mechanical performance of hierarchical cores. Furthermore, recent work on stretch-bend-hybrid hierarchical structures with foam sandwich struts also demonstrates this point [11].

6. Conclusions

In order to increase specific compressive strength of engineering lattice materials, a stretch–stretch-hybrid hierarchical sandwich core was developed, by assembling hollow CPL sandwiches in a pyramidal truss configuration. A practical protocol was presented to evaluate structural efficiency, and following this protocol, experiments and analysis of critical mechanical properties were carried out. Prototype specimens yielded strength values similar to predicted values, demonstrating the utility of the analysis.

Optimization of the hierarchical CPL core was conducted based on collapse mechanism maps, and structural efficiency was evaluated by comparing with other common CPL cores. Effects of the topology or shape in both macroscopic and mesoscopic scales were discussed. The principle findings include:

(1) The structural efficiency of hierarchical structures was affected by the ratio of strut length at different scales (e.g. L/l_1). With the specific limited L/l_1, the hierarchical CPL core was almost 5 times stronger than the corresponding CPL core with rectangular trusses (at relative density 0.01).
(2) The fully optimized hierarchical CPL cores can be as efficient as optimized CPL cores with hollow trusses, and also outperform other traditional lower-order CPL cores.
(3) The efficiency of a given topology at macroscopic length scales determined that of the corresponding hierarchical construction, while topology or truss shape at mesoscopic length scales has little effect on efficiency of an optimized hierarchical construction.

Acknowledgements

The present work is supported by NSFC (90816024 and 10872059), 973 Program (No. 2011CB610303). S.N. gratefully acknowledges support from the Gill Composites Center. S.Y. also acknowledges the support of Most Potential New Scholar Prize awarded by Ministry of Education in China (AUDQ1010000511).

References

[1] Evans AG, Hutchinson JW, Fleck NA, Ashby MF, Wadley HNG. The topological design of multifunctional cellular metals. Progr Mater Sci 2001;46(3–4):309–27.
[2] Wang B, Wu LZ, Ma L, Sun YG, Du SY. Mechanical behavior of the sandwich structures with carbon fiber-reinforced pyramidal lattice truss core. Mater Des 2010;31(5):2659–63.
[3] Queheillalt DT, Wadley HNG. Titanium alloy lattice truss structures. Mater Des 2009;30(6):1966–75.
[4] Sugimura Y. Mechanical response of single-layer tetrahedral trusses under shear loading. Mech Mater 2004;36(8):715–21.
[5] Pingle SM, Fleck NA, Deshpande VS, Wadley HNG. Collapse mechanism maps for the hollow pyramidal core of a sandwich panel under transverse shear. Int J Solids Struct 2011;48(25–26):3417–30.
[6] Lee YH, Lee BK, Jeon I, Kang KJ. Wire-woven bulk Kagome truss cores. Acta Mater 2007;55(18):6084–94.
[7] Lakes R. Materials with structural hierarchy. Nature 1993;361(6412):511–5.
[8] Yin S, Wu L, Nutt S. In-plane compression of hollow composite pyramidal lattice sandwich columns. J Compos Mater 2013. http://dx.doi.org/10.1177/0021998313485309.
[9] Yin S, Wu L, Ma L, Nutt S. Pyramidal lattice sandwich structures with hollow composite trusses. Compos Struct 2011;93(12):3104–11.
[10] Yin S, Wu L, Ma L, Nutt S. Hybrid truss concepts for carbon fiber composite pyramidal lattice structures. Compos Part B-Eng 2012;43(4):1749–55.
[11] Yin S, Wu L, Nutt S. Stretch-bend-hybrid hierarchical composite pyramidal lattice cores. Compos Struct 2013;98:153–9.
[12] Schaedler TA, Jacobsen AJ, Torrents A, Sorensen AE, Lian J, Greer JR, et al. Ultralight metallic microlattices. Science 2011;334(6058):962–5.
[13] Fratzl P, Weinkamer R. Nature's hierarchical materials. Prog Mater Sci 2007;52(8):1263–334.
[14] Ritchie RO. The conflicts between strength and toughness. Nat Mater 2011;10(11):817–22.
[15] Kooistra GW, Deshpande V, Wadley HNG. Hierarchical corrugated core sandwich panel concepts. J Appl Mech-T ASME 2007;74(2):259–68.
[16] Kazemahvazi S, Zenkert D. Corrugated all-composite sandwich structures. Part 1: modeling. Compos Sci Technol 2009;69(7–8):913–9.
[17] Cote F, Russell BP, Deshpande VS, Fleck NA. The through-thickness compressive strength of a composite sandwich panel with a hierarchical square honeycomb sandwich core. J Appl Mech-T ASME 2009;76(6).
[18] Deshpande VS, Fleck NA, Ashby MF. Effective properties of the octet-truss lattice material. J Mech Phys Solids 2001;49(8):1747–69.
[19] Budiansky B. On the minimum weights of compression structures. Int J Solids Struct 1999;36(24):3677–708.